Journal of Fluorescence, Vol. 10, No. 4, 2000

Monitoring the Phase Transition of $C_{12}E_5$/Water/Alkane Microemulsions Through Excimer Formation

M. E. C. D. Real Oliveira,[1,3] Graham Hungerford,[1] E. M. S. Castanheira,[1] M. da G. Miguel,[2] and H. D. Burrows[2]

Received September 28, 1999; revised April 13, 2000; accepted April 17, 2000

The phase transition of microemulsions involving the nonionic surfactant $C_{12}E_5$ [$C_{12}H_{25}(OCH_2$-$CH_2)_5OH$], water, and alkanes (heptane, decane and tetradecane) has been investigated through the excimer formation of pyrene. On going to the microemulsion bicontinuous phase, by changing either composition or temperature, pronounced changes in the pyrene excimer-to-monomer fluorescence intensity ratio, I_E/I_M, are observed. Several differences in the steady-state emission spectra and in fluorescence decay curves show that as a probe pyrene is well suited to follow the transition from the water continuous to the oil continuous phase, through an intermediate bicontinuous (continuous in both water and oil) region. The results provide information about the different characteristics and structure of these three regions (water continuous, bicontinuous, and oil continuous) of the phase diagram for $C_{12}E_5$/water/alkane systems.

KEY WORDS: Nonionic surfactant; microemulsion; excimer; pyrene; phase transition.

INTRODUCTION

It is well known that, under certain conditions of composition and temperature, three component surfactant/oil/water systems may form phases, which are simultaneously continuous in both water and oil [1–3]. The phase diagrams of these three component systems have been extensively studied, and information on them obtained by techniques such as small-angle X-ray and neutron scattering [4, 5], NMR self diffusion [5–8], freeze fracture electron microscopy [5], electrical conductivity [5], viscosity, and surface tension measurements [9]. However, there is interest in obtaining more information at the microscopic level.

[1] Departamento de Física, Universidade do Minho, 4700-320 Braga, Portugal.
[2] Departamento de Química, Universidade de Coimbra, 3049 Coimbra, Portugal.
[3] To whom correspondence should be addressed. e-mail: beta@fisica.uminho.pt

The phase behavior, microstructure, and interactions in nonionic surfactant/water/oil systems, comprising penta (ethylene oxide) dodecyl ether ($C_{12}E_5$) and decane have recently been investigated [10]. Although the microemulsion region has been studied by small-angle neutron scattering [11], there is still a lack of understanding of the factors leading to the transition of water continuous to oil continuous, through a bicontinuous region.

In this work, we have used the fluorescent probe pyrene to monitor the phase changes and structural modification of the system $C_{12}E_5$/water/C_nH_{2n+2} (where n = 7, 10, 14). Because of the ability of pyrene to form excimers through a diffusion-controlled process, this is a valuable probe with which to follow these phase transitions. The excimer formation process has been extensively applied to study microviscosity and molecular interactions in surfactant aggregates [12–14]. We have been interested in applying this technique to obtain a deeper understanding of these three phases, especially the bicontinuous phase in the $C_{12}E_5$/water/alkane system.

1053-0509/00/1200-0347$18.00/0

EXPERIMENTAL

Materials

Samples of polyoxyethylene 5 lauryl ether ($C_{12}E_5$) from Sigma and Nikko Co. Japan were used as received. No differences were observed between the two samples. Pyrene (Koch Light; >99% pure) was zone refined (100 steps). Solutions were prepared using spectroscopic grade solvents and Milli-Q water. The purity of solvents was checked by UV/vis absorption and fluorescence spectroscopy measurements.

Sample Preparation

The samples for the ternary systems were prepared by combining solutions of 16.6% $C_{12}E_5$ in water with 16.6% $C_{12}E_5$ in alkane (C_nH_{2n+2}) to provide the desired weight fraction (x) of alkane, $x = C_nH_{2n+2}/(H_2O + C_nH_{2n+2})$. This solution was then added to a fluorescence cuvette in which the selected amount of pyrene had been deposited by evaporation of a stock solution of pyrene in ethanol. Cuvettes containing the samples were placed in an ultrasonic bath for mixing and after removed and left to stabilize.

Fluorescence Measurements

Steady-state fluorescence spectra of aerated samples were recorded using a Spex Fluorolog spectrofluorimeter. The temperature was maintained (± 0.2°C) using a recirculating water supply connected to a water jacket on the cuvette holder.

The time-resolved fluorescence measurements were made using a single-photon counting spectrometer. This was equipped with a coaxial flashlamp [15] excitation source filled with a nitrogen/hydrogen gas mixture. The excitation wavelength was selected using a 340-nm interference filter (10-nm bandpass). The emission wavelength (393 nm for the monomer and 470 nm for the excimer decays) was selected using a double monochromator with a 16-nm bandpass and the detection was performed with a Philips XP2020Q photomultiplier. The samples were degassed prior to measurement by bubbling with nitrogen. Again, the temperature was maintained using a water-jacketed cuvette holder. The data were analyzed using a nonlinear least-squares analysis (IBH Consultants Ltd.) and the goodness of fit judged in terms of a χ^2 value and weighted residuals.

RESULTS AND DISCUSSION

Steady-State Fluorescence Measurements

Fluorescence spectra were recorded for 10^{-3} M pyrene in 16.6% $C_{12}E_5$/water/tetradecane mixtures at various temperatures. The samples exhibited both single-phase and two-phase regions, in agreement with published phase diagrams [4,6]. However, we concentrate on three separate parts of the single-phase region: (a) the water continuous region (low temperature for constant composition or high water content), corresponding to the L_1 phase of normal micelles swelled with oil; (b) a narrow intermediate region, with an aqueous continuous phase, which is also continuous in oil; and (c) an oil continuous region (high temperature for constant composition or high oil content) corresponding to a water-in-oil microemulsion.

In the three regions, both monomer and excimer emissions are observed (Fig. 1), the latter band was centred at 470 nm. In the bicontinuous phase ($x = 0.45$, 45°C) the excimer emission intensity is markedly lower than in either the oil continuous ($x = 0.9$; 57°C) or the water continuous ($x = 0.1$; 34°C) regions. Figure 2 displays the excimer-to-monomer fluorescence intensity ratio, I_E/I_M, of 10^{-3} M pyrene along the single-phase region of the system 16.6% $C_{12}E_5$/water/tetradecane, on changing the oil fraction and temperature. The pronounced decrease in I_E/I_M in the bicontinuous region shows that pyrene excimer formation is sensitive to these phase transitions. This trend in I_E/I_M is not a temperature effect, since in pure alkanes (Fig. 3), the effect of temperature on the I_E/I_M ratio is in the opposite sense to that observed in the bicontinuous phase. In the water-rich region, $C_{12}E_5$ forms spherical micelles swollen with oil, with a hydrodynamic radius of 80 Å [10]. Because of its hydrophobic character, it is expected that pyrene is situated within the micelles. Evidence for the location of the probe comes from the fluorescence intensity ratio of the vibronic bands of pyrene (10^{-5} M), I_1 ($0 \leftarrow 0$) and I_3 ($2 \leftarrow 0$), which increases with polarity [16]. For the water continuous region ($x = 0.1$; 34°C), $I_1/I_3 = 1.025$, while for pure $C_{12}E_5$, this value is 1.24. These can be compared with values of 1.87 and 0.59 for water and tetradecane, respectively [16]. This indicates that pyrene is located near to the $C_{12}E_5$ molecules. If we consider an aggregation number of 1000, from the data in Refs. 10 and 17 we estimate that on average there are 2.1 molecules of pyrene per micelle. This high local pyrene concentration can justify the larger I_E/I_M value found for the water continuous, compared with the bicontinuous region. For the oil continuous region ($x = 0.9$; 57°C), pyrene is located mainly near the alkyl chains of the surfactant, in contact

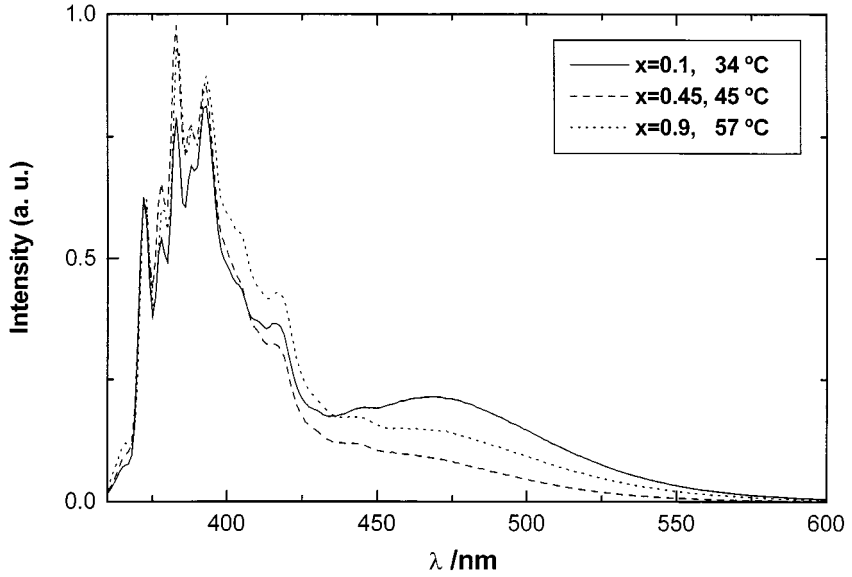

Fig. 1. Normalized emission spectra of 10^{-3} *M* pyrene in 16.6% $C_{12}E_5$/water/tetradecane mixtures: (——) water continuous region, (- - -) bicontinuous region, and (·····) oil continuous region.

with oil, as inferred from the I_1/I_3 value (0.75). In this region, the I_E/I_M value is higher than that observed in the bicontinuous region. Possible explanations are discussed later.

The variation of I_E/I_M observed in Fig. 2 strongly suggests that, in the bicontinuous region, pyrene is located mainly in the oil channels and associated surfactant tails ($I_1/I_3 = 0.80$). In these oil-rich domains, the local concen-

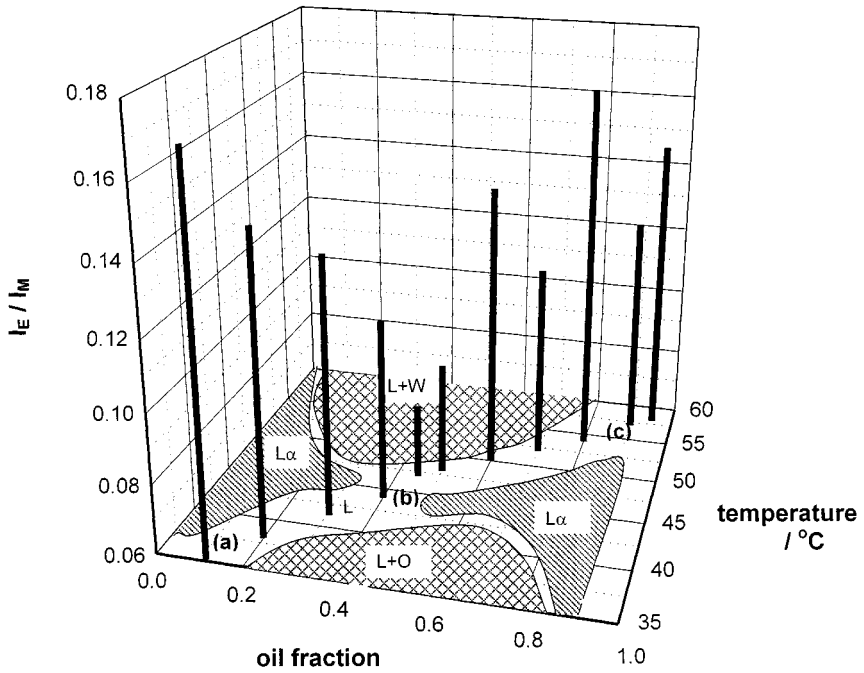

Fig. 2. Excimer-to-monomer fluorescence intensity ratio, I_E/I_M, of pyrene (10^{-3} *M*) along the single-phase region of the system 16.6% $C_{12}E_5$/water/tetradecane. The phase diagram was adapted from Ref. 4.

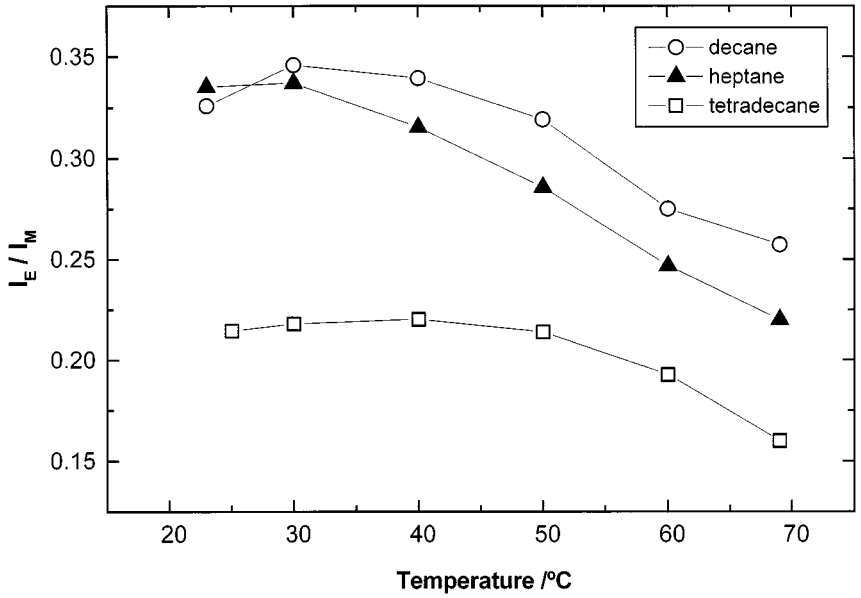

Fig. 3. Variation with temperature of the excimer-to-monomer fluorescence intensity ratio, I_E/I_M, for pyrene (10^{-3} *M*) in heptane, decane, and tetradecane.

tration of pyrene is expected to be lower than in the other regions, and the probability of that pyrene monomers form a dynamic excimer by a diffusive process is very small. This fact is borne out by the low I_E/I_M value observed in the bicontinuous region.

Further information of the probe location comes from the position of the excimer band for the three regions under study. On going from the water continuous to the bicontinuous region, the excimer band exhibits a significant blue-shift, as shown in Fig. 4. This blue-shift can be readily explained by a decrease in polarity of the medium surrounding the excimer [18]. Furthermore, the excimer band position is essentially the same in both the bicontinuous and the oil continuous

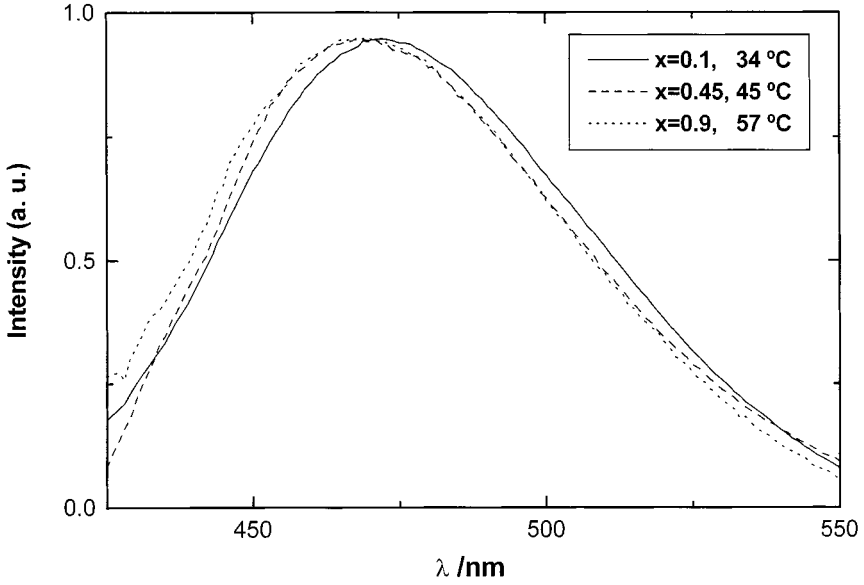

Fig. 4. Normalized pyrene excimer bands in 16.6% $C_{12}E_5$/water/tetradecane mixtures: (——) water continuous region, (- - -) bicontinuous region, and (·····) oil continuous region. Excimer spectra were obtained by subtraction of the monomer spectra (emission of 10^{-5} *M* pyrene in each region of the $C_{12}E_5$/water/tetradecane system) from the global spectra presented in Fig. 1.

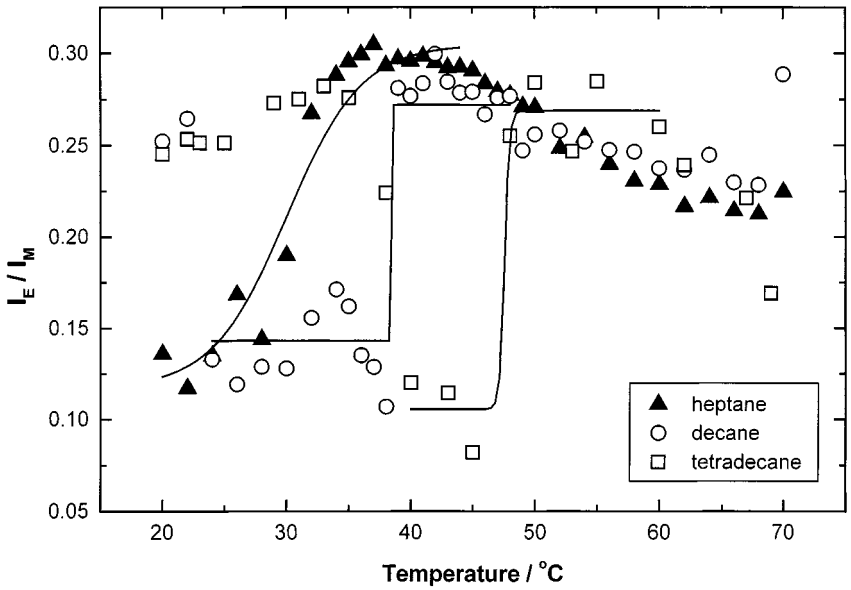

Fig. 5. Excimer-to-monomer fluorescence intensity ratio, I_E/I_M, of 10^{-3} *M* pyrene in 16.6% $C_{12}E_5$/water/alkane systems on cooling from two phases → one phase → two phases. Data were fitted to Boltzmann sigmoidal curves (Microcal Origin) and transition temperatures mentioned in text are taken as the half-height values.

regions, suggesting the same excimer environment in these two regions. The magnitude of the observed blue shift is too big to be explained simply by temperature variation [19].

A study of the system 16.6% $C_{12}E_5$/water/alkane was performed at constant composition ($x = 0.45$) as a function of temperature. These systems, on cooling, pass from a two-phase region (water-in-oil microemulsions + water) to a single bicontinuous microemulsion over a certain temperature range, and then to a second two-phase region (oil-in-water microemulsions + oil) [6]. Solutions were heated to 70°C and the emission spectrum was recorded at various temperatures on cooling. In all cases, a sharp decrease in the excimer-to-monomer intensity ratio was observed, at temperatures corresponding to the transition to the single-phase bicontinuous region. The transition temperature depends on the alkane chain length, with values of about 30°C for heptane. 38°C for decane, and 47.5°C for tetradecane (Fig. 5). The I_E/I_M ratio obtained in the bicontinuous region is similar for the three alkanes.

Time-Resolved Fluorescence Measurements

To complement the information from the steady-state fluorescence measurements, a time-resolved study of pyrene in the three regions was performed.

In homogeneous media, the processes involving monomer–excimer kinetics can be described by the classical Birks scheme (Scheme I) [20], if ground-state dimer formation and transient effects are negligible. Scheme I predicts that, after a δ-pulse of excitation light, the monomer decays as a sum of two exponentials and the excimer as a difference of two exponentials [20],

$$I_M(t) = a_1\exp(-\lambda_1 t) + a_2\exp(-\lambda_2 t) \quad (1)$$

$$I_E(t) = a_3\exp(-\lambda_1 t) - a_4\exp(-\lambda_2 t) \quad (2)$$

where the decay constants λ_1 and λ_2 are given by

$$2\lambda_{1,2} = (A_x + A_y) \mp \sqrt{(A_x - A_y)^2 + 4k_1 k_{-1}[M]} \quad (3)$$

with

$$A_x = k_M + k_1[M] \quad \text{and} \quad A_y = k_E + k_{-1} \quad (4)$$

The preexponential factor ratios for monomer and excimer decay are, respectively,

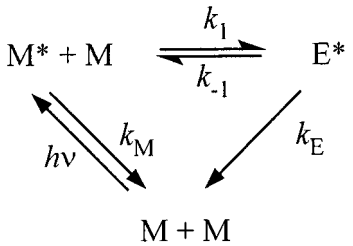

Scheme I. k_1 and k_{-1} are the rate constants for excimer formation and dissociation, respectively. k_M and k_E are the rate constants for monomer and excimer deactivation, respectively.

$$\frac{a_2}{a_1} = \frac{A_x - \lambda_1}{\lambda_2 - A_x} \qquad \text{and} \qquad \frac{a_4}{a_3} = 1 \tag{5}$$

From the values of the decay constants, λ_1, λ_2 and the ratio a_2/a_1, all the relevant kinetic parameters (k_1, k_{-1}, and k_E) can be calculated once the monomer lifetime, $\tau_M = 1/k_M$, is known. The τ_M values are obtained from the monoexponential decay curves of dilute solutions of pyrene (10^{-5} *M*) in the three regions under study.

In all cases, for degassed solutions of 10^{-3} *M* pyrene, the excimer decay curves can be fitted as the difference of two exponentials, with a ratio of preexponential factors (a_4/a_3) close to 1. This indicates that the formation of pyrene dimers in the ground state is not observed in the three regions. The monomer decay curves can be fitted as a sum of two exponentials, and in both the bicontinuous ($a_1 = 0.03$, $\tau_1 = 16.6$ ns; $a_2 = 0.97$, $\tau_2 = 201.3$ ns; $\chi^2 = 1.25$) and the oil continuous regions ($a_1 = 0.05$, $\tau_1 = 19.9$ ns; $a_2 = 0.95$, $\tau_2 = 214.7$ ns; $\chi^2 = 0.99$), the recovered lifetime values are very close to those obtained from the excimer decay. In the water continuous region, lifetimes from the monomer decay differ significantly from those of the excimer decay (Fig. 6). In this region, unlike the bicontinuous and oil-rich regions, the pyrene is confined to micellar aggregates. From simple pyrene distribution considerations, it is likely that there are aggregates in which excimer formation does not occur. This will obviously influence the monomer decay.

To estimate the rate constants for excimer formation and dissociation, k_1 and k_{-1}, in the water continuous region, the value of k_E was fixed to that obtained in pure tetradecane at the same temperature. This makes it possible to calculate k_1 and k_{-1} from the excimer decay lifetimes, without recourse to the monomer decay preexponential factors. The rate constants k_1, k_{-1}, and k_E calculated for the three regions are presented in Table I. For comparison, the same parameters for 10^{-3} *M* pyrene in pure tetradecane at each temperature are also shown.

The rate constants in the bicontinuous and oil continuous regions are very close to those calculated in pure tetradecane at the same temperatures. This strongly suggests that pyrene is in contact with the oil domain. However, a rather different behavior is obtained in the water continuous region, where the rate constants for excimer formation and dissociation are significantly greater than in tetradecane. This can be explained from the pyrene distribution, where some micelles will contain more than two pyrene molecules. The higher local concentration of pyrene is expected to play an important role, with much faster formation of excimer in micelles with several molecules of pyrene. Furthermore, the larger excimer dissociation rate can enhance the existence of geminate pairs,

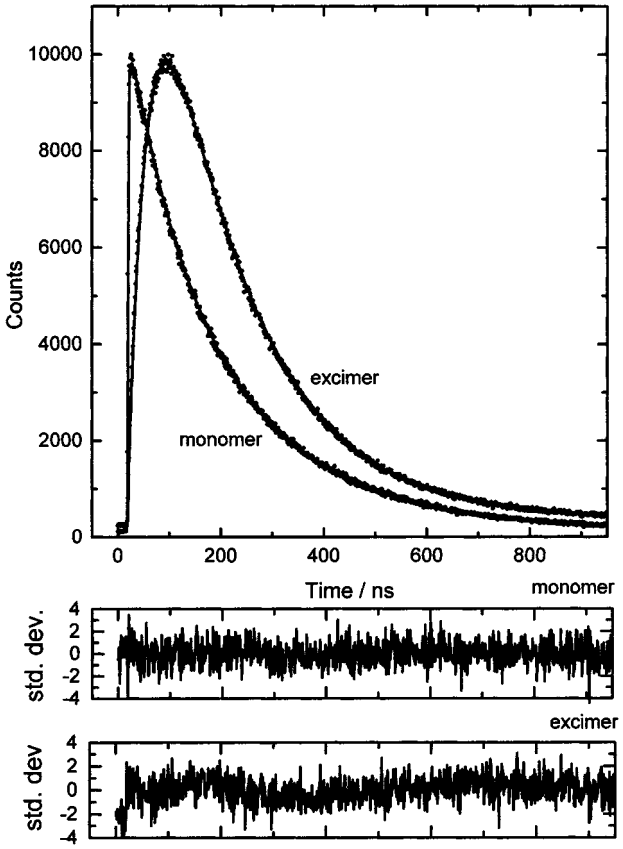

Fig. 6. Fluorescence decay curves of excimer and monomer of 10^{-3} *M* pyrene in 16.6% $C_{12}E_5$/water/tetradecane system in the water continuous region at 34°C fitted with a sum of two exponentials. The recovered fit values are as follows: excimer, $a_1 = -0.49$, $\tau_1 = 39.9$ ns, and $a_2 = 0.51$, $\tau_2 = 167.2$ ns ($\chi^2 = 1.23$); monomer, $a_1 = 0.24$, $\tau_1 = 88.4$ ns, and $a_2 = 0.76$, $\tau_2 = 204.4$ ns ($\chi^2 = 1.19$). The weighted residuals for each fit are also given.

Table I. Rate Constants for Excimer Formation, Dissociation, and Deactivation of Pyrene in the 16.6% $C_{12}E_5$/Water/Tetradecane System and in Pure Tetradecane

	k_1 (M^{-1} s^{-1})	k_{-1} (s^{-1})	k_E (s^{-1})
Region			
Water continuous ($x = 0.1$; 34°C)	3.5×10^9	6.7×10^6	1.7×10^{7a}
Bicontinuous ($x = 0.45$; 45°C)	2.3×10^9	1.7×10^7	1.7×10^7
Oil continuous ($x = 0.9$; 57°C)	2.6×10^9	3.8×10^7	1.02×10^7
Pure tetradecane			
34°C	1.7×10^9	5.8×10^6	1.7×10^7
45°C	2.2×10^9	1.8×10^7	1.7×10^7
57°C	2.6×10^9	4.0×10^7	1.5×10^7

[a] Fixed.

which can recombine faster than the initial excited monomers [21].

CONCLUSION

In this work, we have shown that pyrene is a well-suited probe to follow the transition from a water continuous to an oil continuous region in the system $C_{12}E_5$/water/alkane. Pronounced changes are observed in the pyrene excimer-to-monomer fluorescence intensity ratio, especially on traversing the intermediate bicontinuous domain. These changes are also manifest in the time-resolved behavior of the probe.

ACKNOWLEDGMENTS

G.H. would like to thank the Fundação para a Ciência e a Tecnologia (PRAXIS XXI) for financial support, as would M. da G.M. and H.D.B. (Project 2/2.1/QUI/411/94).

REFERENCES

1. L. E. Scriven (1976) *Nature* **263**, 123–125.
2. B. Lindman, N. Kamenka, T.-M. Kathopoulis, B. Brun, and P.-G. Nillson (1980) *J. Phys. Chem.* **84**, 2485–2490.
3. U. Olsson and H. Wennerstrom (1994) *Adv. Colloid Interface Sci.* **49**, 113–146.
4. F. Lichterfeld, T. Schmeling, and R. Strey (1986) *J. Phys. Chem.* **90**, 5762–5766.
5. M. Kahlweit, R. Strey, D. Haase, H. Kunieda, T. Schmeling, B. Faulhaber, M. Borkovec, H.-F. Eixke, G. Busse, F. Eggers, Th. Funck, H. Richman, L. Magid, O. Soderman, P. Stilbs, J Winkler, A. Dittrich, and W. Jahn (1987) *J. Colloid Interface Sci.* **118**, 436–453.
6. U. Olsson, K. Shinoda, and B. Lindman (1986) *J. Phys. Chem.* **90**, 4083–4088.
7. U. Olsson, K. Nagai, and H. Wennerstrom (1988) *J. Phys. Chem.* **92**, 6675–6679.
8. M. Leaver, I. Furó, and U. Olsson (1995) *Langmuir* **11**, 1524–1529.
9. U. Olsson, U. Wurz, and R. Strey (1993) *J. Phys. Chem.* **97**, 4535–4539.
10. H. Bagger-Jörgensen (1997) *Polymer Effects on Microemulsions and Lamellar Phases*, Ph.D. thesis. Lund University, Lund, and references therein.
11. H. Bagger-Jörgensen, U. Olsson, and K. Mortensen (1997) *Langmuir* **13**, 1413–1421.
12. H. J. Pownall and L. C. Smith (1973) *J. Am. Chem. Soc.* **95**, 3136–3140.
13. K. Kalyanasundaraman, M. Grátzel, and J. K. Thomas (1975) *J. Am. Chem. Soc.* **97**, 3915–3922.
14. R. Parthasarathy and M. M. Labes (1990) *Langmuir* **6**, 542–547.
15. D. J. S. Birch and R. E. Imhof (1981) *Rev. Sci. Instrum.* **52**, 9–15.
16. D. C. Dong and M. A. Winnik (1984) *Can. J. Chem.* **62**, 2560–2565.
17. B. Lindman, F. Tiberg, L. Piculell, U. Olsson, P. Alexandridis, and H. Wennerström (1998) in D. O. Shah (Ed.), *Micelles, Microemulsions and Monolayers—Science and Technology*, Marcel Dekker, New York, pp. 101–126.
18. E. M. S. Castanheira and J. M. G. Martinho (1991) *Chem. Phys. Lett.* **185**, 319–323.
19. E. M. S. Castanheira and J. M. G. Martinho (1993) *Chem. Phys. Lett.* **206**, 45–48.
20. J. B. Birks, D. J. Dyson, and I. H. Munro (1963) *Proc. Roy. Soc. A* **275**, 575–588.
21. A. T. Reis e Sousa, E. M. S. Castanheira, A. Fedorov, and J. M. G. Martinho (1998) *J. Phys. Chem. A* **102**, 6406–6411.